

# Theoretical Calculations on Hydrogenase Kinetics: Explanation of the Lag Phase and the Enzyme Concentration Dependence of the Activity of Hydrogenase Uptake

Judit Ósz, Gabriella Bodó, Rui Miguel Mamede Branca, and Csaba Bagyinka

Institute of Biophysics, Biological Research Center of the Hungarian Academy of Sciences, H-6701, Szeged, Hungary

**ABSTRACT** Two models of the hydrogenase reaction cycle were investigated by means of theoretical calculations and model simulations. The first model is the widely accepted triangular hydrogenase reaction cycle with minor modifications; the second is a modified triangular model, where we have introduced an autocatalytic step into the reaction cycle. Both models include a one-step activation reaction. The theoretical calculations and model simulations corroborate the assumed autocatalytic reaction step concluded from the experimental characteristics of the hydrogenase reaction.

## INTRODUCTION

Hydrogenases are metalloenzymes that catalyze the reaction  $H_2 \rightleftharpoons 2 H^+ + 2 e^-$ . Although the enzymatic activity of hydrogenase is determined routinely, a number of contradictory results have been published. Despite the many features that have been described in the hydrogenase reaction, the activity of this class of enzymes has not yet been thoroughly explained (1–9). However, there is a consensus in the hydrogenase literature that the reaction is linear; no feedback from any parts of the reaction occurs, except that some authors admit that there might be a nonlinear feedback during the activation of the enzyme (9–11).

Several models of the hydrogenase reaction have been published, based on equilibrium or quasiequilibrium states of hydrogenase derived from redox titration and measured by electron paramagnetic resonance and/or infrared (IR) spectroscopy (7–9,12). The various models can be condensed into two different models, the main characteristics of which are outlined in Fig. 1.

Both models include a double activation chain. Two inactive forms of hydrogenase, Form A ( $Ni_a-A_{1945}^*$  in Fig. 1) and Form B ( $Ni_b-B_{1943}^*$  in Fig. 1), can be activated through several intermediates. The enzyme reaction cycle involves three hydrogenase forms,  $Ni_a-S_{1931}$  (Form S),  $Ni_a-C_{1950}^*$  (Form C), and  $Ni_a-SR_{1936}$  (Form SR). These three hydrogenase forms participate in the enzyme reaction cycle in the triangular model (6–8), whereas there are two enzyme reaction cycles in the other model (9), each cycle involving two enzyme forms (Form S/Form C and Form C/Form SR cycles), Form C being common in the two cycles.

We recently demonstrated that the hydrogenase catalytic reaction includes at least one autocatalytic step (13–15). This assumption was based on the special patterns of the hydrogenase-uptake reaction in a thin-layer reaction chamber and

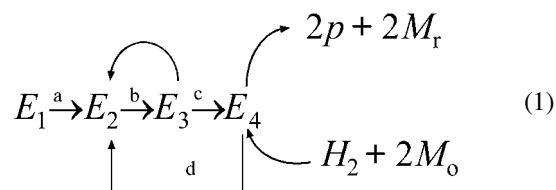
on the autocatalytic oscillations in the fast absorption kinetics of the methyl viologen-initiated reaction of hydrogenase. The assumption of an autocatalytic step explains most of the contradictory findings in previous publications.

We now report a detailed kinetic simulation of the hydrogenase-uptake reaction, based on a commonly accepted hydrogenase kinetic model (the triangular model described above) and on a slightly modified model, where we introduce an autocatalytic step into the triangular model. Such model calculations are not to be found in the literature, though they can shed light on the measured kinetic characteristics of the enzyme reaction.

## MATERIALS AND METHODS

### Theoretical calculations

Ordinary differential equations (ODEs) were solved numerically by using the computer program Maple V Release 4 under the Warp 4 operating system on a commercial PC, and/or the program Maple V Release 5 under the IRIX operating system on a Silicon Graphics Origin 2000 (Mountain View, CA) computer. We always used the “stiff” solvers (lsode or gear) when simulating the kinetic curves.



In most of the theoretical calculations, the kinetic model presented in Eq. 1 was used. This is a slightly modified version of the triangular model (6–8). The first and most significant simplification was to regard all reactions as unidirectional: only the hydrogen-uptake direction was taken into account. Secondly, the hydrogen uptake and proton/electron release were incorporated into a single catalytic step. We condensed all activation reactions into a single one (a); consequently, only one inactive form of hydrogenase is present in the model ( $E_1$ ).

The modifications are partly due to the limitations of the ODE subroutine widely used for solving differential equations, and computer memory, because of which we had to simplify the hydrogenase-uptake reaction. The

Submitted January 8, 2005, and accepted for publication May 11, 2005.

Address reprint requests to Csaba Bagyinka, Temesvári krt. 62, Szeged, PO Box 521, H-6701, Hungary. Tel.: 36-62-599605; Fax: 36-62-433133; E-mail: csaba@nucleus.szbk.u-szeged.hu.

© 2005 by the Biophysical Society

0006-3495/05/09/1957/08 \$2.00

doi: 10.1529/biophysj.105.059246

autocatalytic model is very time and memory consuming to simulate. In some cases, two other models were also used, in both autocatalytic and conventional form. One was the full model containing a double activation chain according to the triangular model. In the other model that we developed, we extended the hydrogen splitting into separate steps. The kinetic simulations did not demonstrate any significant qualitative difference in the results. We concluded, that the simplification of the model did not alter the main characteristics of the calculated kinetics, and therefore the calculations of the simplified model have been used throughout the publication.

If Eq. 1 is compared with the triangular model (Fig. 1 A),  $E_2$  corresponds to the  $\text{Ni}_a\text{-S}_{1931}$  state,  $E_3$  to  $\text{Ni}_a\text{-C}_{1950}$  (Form C), and  $E_4$  to  $\text{Ni}_a\text{-SR}_{1936}$  (Form SR). The substrates of the reaction are  $M_o$  (oxidized methyl viologen) and  $H_2$  (hydrogen gas), whereas the products are protons ( $p$ ) and reduced methyl viologen ( $M_r$ ).

Throughout the calculations we have used micromolars to express concentrations and seconds to express time. These units are arbitrary for the calculations, though the numerical values of the parameters chosen are very close to the experimentally observed numbers. We varied the kinetic parameters ( $a$ ,  $b$ ,  $c$ , and  $d$ ) to obtain a reasonable computation time and time courses as close as possible to the experimental values.

The set of differential equations for the modified triangular model is as follows:

$$\begin{aligned} \dot{E}_1 &= -aE_1 \\ \dot{E}_2 &= +aE_1 - bE_2 + dE_4H_2M_o^2 \\ \dot{E}_3 &= +bE_2 - cE_3 \\ \dot{E}_4 &= cE_3 - dE_4H_2M_o^2 \\ \dot{H}_2 &= -dE_4H_2M_o^2 \\ \dot{M}_0 &= -2dE_4H_2M_o^2 \\ \dot{M}_r &= +2dE_4H_2M_o^2 \end{aligned} \quad (2)$$

which changes in the case of the autocatalytic enzyme cycle to

$$\begin{aligned} \dot{E}_1 &= -aE_1 \\ \dot{E}_2 &= +aE_1 - bE_2/E_3 + dE_4H_2M_o^2 \\ \dot{E}_3 &= +bE_2/E_3 - cE_3 \\ \dot{E}_4 &= cE_3 - dE_4H_2M_o^2 \\ \dot{H}_2 &= -dE_4H_2M_o^2 \\ \dot{M}_0 &= -2dE_4H_2M_o^2 \\ \dot{M}_r &= +2dE_4H_2M_o^2 \end{aligned} \quad (3)$$

The following definitions are used:  $E_T = E_1 + E_2 + E_3 + E_4$  is the total enzyme concentration,  $E_a = E_2 + E_3 + E_4$  is the active enzyme concentration,  $E_{a0}$  is the active enzyme concentration at  $t = 0$ , and  $E_{10}$  is the inactive enzyme concentration at  $t = 0$ .

The kinetics of both autocatalytic and conventional reactions were calculated and compared. When possible, the differential equations were solved for equilibrium states. The parameters of the reaction were changed systematically to simulate different experimental results. The specific characteristics of the results of the simulations were compared with published experimental findings.

## RESULTS

### Activation of the enzyme

It is known that hydrogenase can be activated if it is incubated under hydrogen (5,16). The activation is a very slow process; to achieve full activation, the enzyme should be incubated for several hours ( $a$  is small,  $\sim 0.001$ – $0.0001$  in the first enzyme reaction). Activation, which changes the distribution of the enzyme forms, can occur only under a hydrogen atmosphere. Activation in a closed IR sample hol-

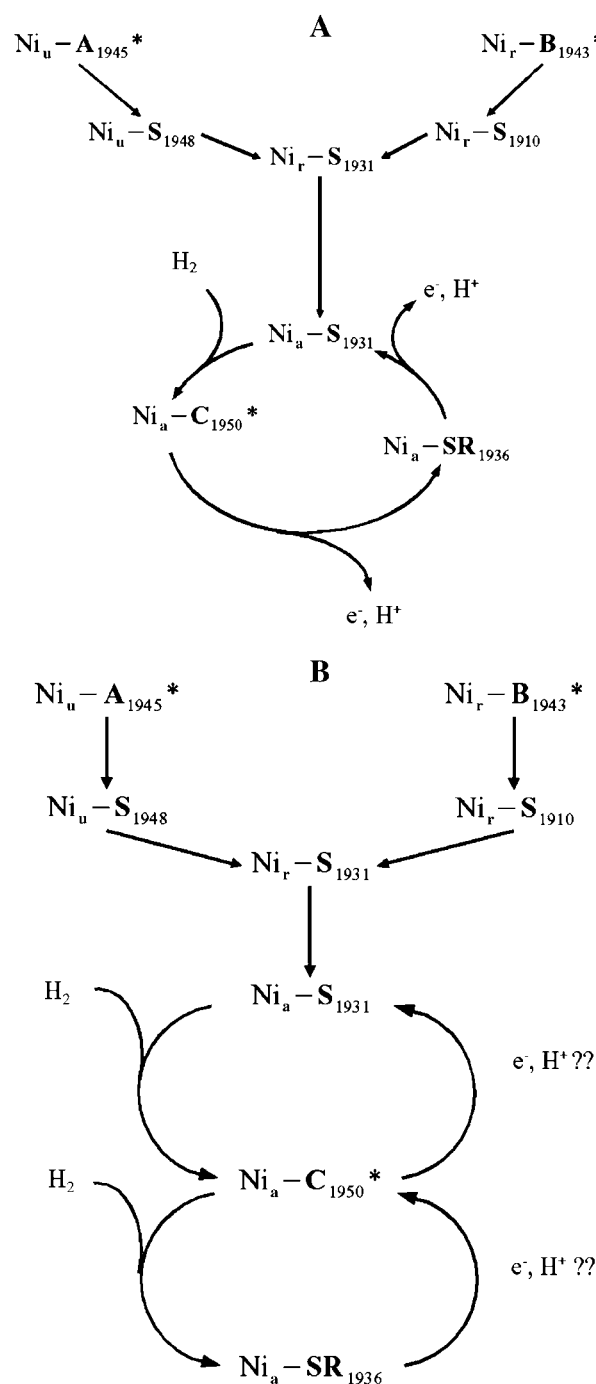


FIGURE 1 Different hydrogenase kinetic models. (A) Triangular kinetic model of hydrogenase reaction. (B) Double-cycle model. For references, see the text.

der is known to result in the accumulation of Form SR (12). We simulated the activation by allowing only the enzyme forms to react; there was no enzyme-substrate reaction. It is evident that a hydrogen reaction should be included in the reaction, but there is no consensus in the literature as to where the hydrogen reacts and what kind of reaction it is. Disregarding substrates, however, does not affect the kinetic

characteristics of the reaction because activation involves merely a redistribution of the enzyme forms, which remains possible in the model.

#### The conventional triangular model

The concentration of  $E_4$  continuously increases in time, revealing an activation process during hydrogen incubation. Activation in our model resulted in the accumulation of  $E_4$ , which is an active enzyme form in the modified triangular model and corresponds to Form SR ( $\text{Ni}_a\text{-SR}_{1936}$  in Fig. 1) of the enzyme, which is in agreement with the observed characteristics (12). Because the initial velocity of the reaction is proportional to the concentration of  $E_4$ , this concentration is presented as a measure of the activation (a measure of the initial enzyme activity). The results of the activation are to be seen in Fig. 2 (labeled as ‘‘all nonautocatalytic’’). The enzyme activation is a monotonous and smooth function of time; no lag phase and no concentration dependence can be observed in the conventional triangular model for the enzyme activation.

#### The autocatalytic triangular model

The results of the activation in the case of autocatalytic triangular model may also be seen in Fig. 2 (curves labeled by numbers, indicating the enzyme concentration). The concentration of  $E_4$  continuously increases in time, indicating an activation process during hydrogen incubation. The results reveal a lag phase in the  $E_4$  concentration. The lag phase increases when the total enzyme concentration is lowered.

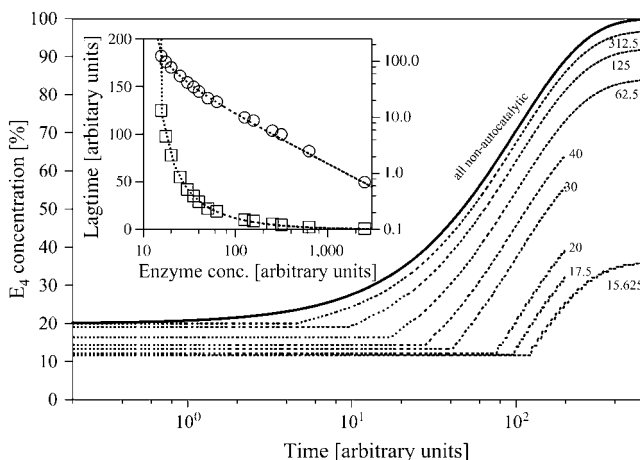


FIGURE 2 Activation of hydrogenase. Theoretical simulation of the activation of hydrogenase using both the nonautocatalytic and the autocatalytic triangular model. Semilog representation. The parameters used for simulation are:  $a = 0.01$ ,  $b = 100$ ,  $c = 1000$ ,  $d = 0$ . The initial distribution of the enzyme forms:  $E_1 = 0.8 \cdot E_T$ ,  $E_2 = 0.1 \cdot E_T$ ,  $E_3 = 0.1 \cdot E_T$ ,  $E_4 = 0$ . The curves reflect specific time courses (values were divided by the total enzyme concentration) at different total enzyme concentrations, as indicated near the curves. (Inset) Enzyme concentration dependence of lag phases in semilog ( $\square$ ) and log-log ( $\circ$ ) representations. The function describing the dependence is a hyperbolic function with the power  $-0.86 \pm 0.03$ .

The lag phase is a hyperbolic function of the enzyme concentration (Fig. 2, inset).

#### Enzyme cycle of the activated enzyme

If the enzyme is fully activated, then  $E_1 = 0$ , and consequently  $E_T \equiv E_{a0} = E_a = E_2 + E_3 + E_4$ . At equilibrium, after transients the concentrations of all the different enzyme forms are constant, and the differential equations can therefore be reduced to simple algebraic equations.

#### The conventional triangular model

In the case of the conventional triangular model, the equilibrium concentrations can be calculated from the set of equations:

$$\begin{aligned} bE_2 &= d'E_4 \\ bE_2 &= cE_3 \\ cE_3 &= d'E_4 \\ E_T &= E_{a0} = E_a = E_2 + E_3 + E_4 \\ \text{where } d' &= dH_2M_0^2. \end{aligned} \quad (4)$$

The enzyme activity can be calculated from the change in the reduced methyl viologen concentration:

$$v = 2d'E_4. \quad (5)$$

If the equation is reduced to known values, the activity of the enzyme after transients and far from the end of the reaction ( $H_2$  and  $M_0$  are nearly constant) is given by:

$$v = \frac{2bcd'}{cd' + bd' + bc} E_{a0}. \quad (6)$$

Because this equation does not yield information about the early phase of the reaction, where equilibrium is not established, we also simulated the early phase of the reaction (Fig. 3). No lag phase or enzyme activity versus enzyme concentration dependence could be observed in this model.

#### The autocatalytic triangular model

Similarly as for the conventional model, the set of differential equations becomes a set of algebraic equations:

$$\begin{aligned} bE_2E_3 &= d'E_4 \\ bE_2E_3 &= cE_3 \\ cE_3 &= d'E_4 \\ E_T &= E_{a0} = E_a = E_2 + E_3 + E_4 \\ \text{where } d' &= dH_2M_0^2. \end{aligned} \quad (7)$$

The enzyme activity can also be calculated from the reduced methyl viologen concentration change:

$$v = 2d'E_4. \quad (8)$$

After substitution, this becomes:

$$v = \frac{2cd'}{d' + c} E_a - \frac{c^2d'}{(d' + c)b} = \frac{2cd'}{d' + c} \left( E_{a0} - \frac{c}{b} \right). \quad (9)$$

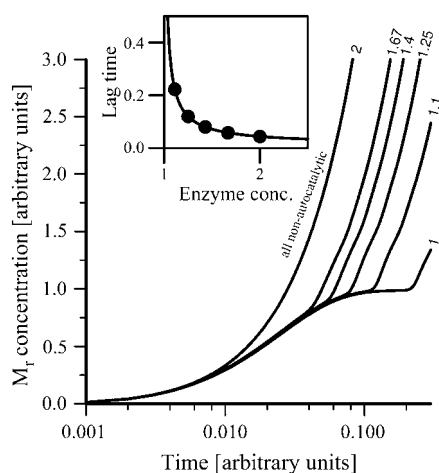


FIGURE 3 Enzyme reaction of fully activated hydrogenase. Theoretical simulation of hydrogenase activity kinetic measurements of fully activated hydrogenase reaction using both the conventional and the autocatalytic triangular model. Semilog representation. The parameters used for simulation:  $a$  = not used,  $b = 1000$ ,  $c = 1000$ ,  $d = 10^{-11}$ . The initial distribution of the enzyme forms, substrates, and products:  $E_1 = 0$ ,  $E_2 = 0.1 \cdot E_T$ ,  $E_3 = 0.9 \cdot E_T$ ,  $E_4 = 0$ ,  $H_{20} = 10^6$ ,  $p_0 = 0$ ,  $M_0 = 2000$ . The curves reflect specific time courses (values were divided by the total enzyme concentration) at different total enzyme concentrations, as indicated near the curves. (Inset) Enzyme concentration dependence of lag phases. The function describing the dependence is a hyperbolic function with the power  $-0.87(2)$ .

The interesting conclusion is that there is a threshold in the enzyme concentration. If the full enzyme concentration (which in this case is the same as the active enzyme concentration) is smaller than  $c/b$ , the reaction will apparently never start. Because we have assumed that the transient phenomena are fast, we cannot say anything definite for the situation below the threshold, where this assumption is obviously not true.

However, we can simulate the whole cycle of the fully activated enzyme. The results are presented in Fig. 3. The reaction also starts with a lag phase. The length of the lag phase in this case, too, depends on the enzyme concentration as a hyperbolic function (Fig. 3, inset).

### Enzyme cycle of the partially active enzyme

In this case,  $E_T = E_{a0} + E_{10}$  and  $E_{10} \simeq E_T \gg E_{a0}$ , i.e., only a small proportion of the enzyme is in the active form. It is also known that  $a$  is very small ( $\sim 0.001$ – $0.0001 \text{ s}^{-1}$ ); the activation of the enzyme requires hours (5,16). Because  $a$  is very small and  $E_{10} \simeq E_T = \text{constant}$ , we can assume that  $aE_1 \simeq aE_{10}$  is constant. The active enzyme form will increase as  $E_a = E_{a0} + aE_{10}t$ .

#### The conventional triangular model

The reaction can be depicted as in the case of the activated enzyme, but with a slow constant increase in the activated form,  $E_a = E_{a0} + aE_{10}t$ . The velocity of the reaction is:

$$v = \frac{2bcd'}{cd' + bd' + bc}(E_{a0} + aE_{10}t). \quad (10)$$

Because  $E_1 \simeq E_{10} = \text{constant}$ , it describes a velocity constantly increasing in time.

We also simulated the above reaction to investigate how the enzyme activity depends on the total enzyme concentration. The results are presented in Fig. 4. The activity is measured as the maximum velocity of the product versus time function determined from the first derivative (Fig. 4 C, bottom curves). It is obvious that the enzyme activity (the maximum velocity) depends strongly on the enzyme concentration. The dependence is best described as a square root function of the enzyme concentration (Fig. 5). No lag phase versus enzyme concentration dependence could be observed in this case.

#### The autocatalytic triangular model

Similarly as for the conventional model, the active enzyme concentration in this case can be depicted as a time-dependent value. The velocity of the reaction becomes:

$$v = \frac{2cd'}{d' + c}E_a - \frac{2c^2d'}{(d' + c)b} = \frac{2cd'}{d' + c}\left(E_{a0} - \frac{c}{b} + aE_{10}t\right), \quad (11)$$

which also constantly increases in time, similarly as in the conventional model. The threshold value still exists in this case:  $E_a = E_{a0} + aE_{10}t$  should be higher than  $c/b$ . There is a considerable difference and a new phenomenon appears, however, if  $E_T$  is greater than the threshold, but  $E_{a0}$  is smaller. When the continuously increasing  $E_a = E_{a0} + aE_{10}t$  reaches the threshold, the reaction velocity becomes positive and the reaction starts. The period during which this happens is the lag phase of the autocatalytic reaction, which can be calculated as:

$$\begin{aligned} E_{a0} - \frac{c}{b} + aE_{10}t_{\text{lag}} &= 0 \\ \text{if } E_{a0} &= pE_T \text{ and } E_1 \simeq E_{10} = (1 - p)E_T = \text{const.} \\ t_{\text{lag}} &= \frac{c}{ab(1 - p)}\left(\frac{1}{E_T} - \frac{bp}{c}\right). \end{aligned} \quad (12)$$

The lag phase of the reaction in this autocatalytic model depends on the enzyme concentration as a hyperbolic function. As the enzyme concentration is increased (at constant  $p$ , which means that the active enzyme concentration increases, too), at a certain point it reaches a threshold, when the lag phase disappears and the reaction starts immediately, as described in the case of the fully activated enzyme.

We also simulated the above reaction to investigate how the enzyme activity depends on the total enzyme concentration. The results are likewise presented in Fig. 4. The activity in this case is also measured as the maximum velocity of the product versus time function determined from the first derivative (Fig. 4 A, bottom curves). Similarly as in the conventional model, the activity of the enzyme depends on the

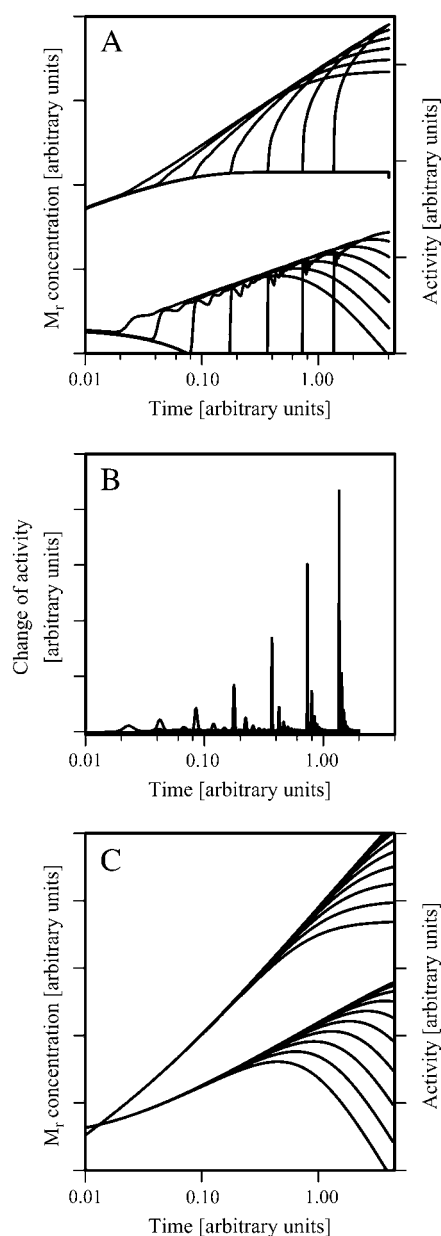


FIGURE 4 Enzyme reaction of partially activated hydrogenase. Theoretical simulation of hydrogenase activity kinetic measurements of partially activated hydrogenase reaction using both the nonautocatalytic and the autocatalytic triangular model. The parameters used for simulation:  $a = 0.001$ ,  $b = 1000$ ,  $c = 1000$ ,  $d = 10^{-10}$ . The initial distribution of the enzyme forms, substrates, and products:  $E_1 = (1 - 0.00002) \cdot E_T$ ,  $E_2 = 0$ ,  $E_3 = 0.00002 \cdot E_T$ ,  $E_4 = 0$ ,  $H_{20} = 10^6$ ,  $p_0 = 0$ ,  $M_0 = 400$ . The curves reflect specific time courses at different total enzyme concentrations. All calculated kinetic values were divided by the enzyme concentration. The activities were calculated by differentiating the time courses. The change in activity was calculated by differentiating the activity curves. (A) Autocatalytic model, log-log representation. (B) Change in activity (second derivative of the kinetics curves) calculated from panel A, semilog representation. (C) Nonautocatalytic model, log-log representation. Top curves in panels A and C are the calculated kinetics; bottom curves in panels A and C are momentary velocities of the reaction.

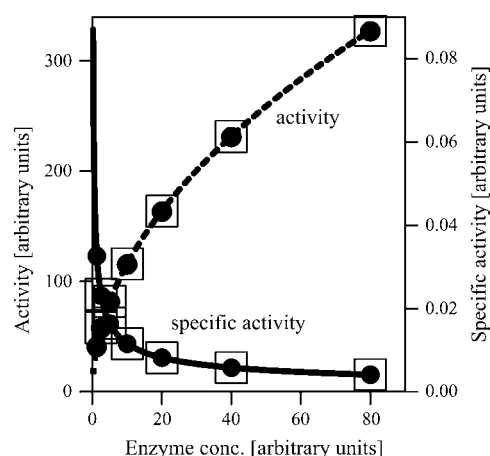


FIGURE 5 The enzyme concentration dependence of the activity and specific activity of partially activated hydrogenase. The data were calculated from the maximum velocity values of Fig. 4. ( $\square$ ) Derived from the autocatalytic model; ( $\bullet$ ) derived from the nonautocatalytic model. The curve is best described as a square-root function of concentration (the power value is 0.4988(5) for the activity and  $-0.5033(5)$  for the specific activity).

enzyme concentration as a square root function (Figs. 4 and 5). There is no difference in this behavior between the autocatalytic and the conventional model.

The second derivative of the kinetics has also been calculated to determine if any peak is observed at the end of the lag phase, as suggested on the basis of the experimental data (15). The calculated second derivative curve is to be seen in Fig. 4 B. A very characteristic peak can be observed at the end of the lag phase. No such peak is present in the case of

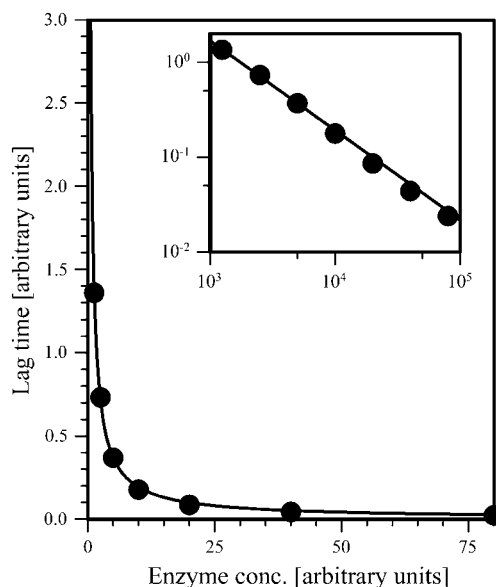


FIGURE 6 Enzyme concentration dependence of lag phase of partially activated hydrogenase. The lag-phase values were calculated from the autocatalytic simulation presented in Fig. 4. The function describing the dependence is a hyperbolic function with the power  $-0.91(3)$ . (Inset) The same curve in log-log representation.

the conventional model (simulation not shown). The lag phase of the reaction calculated from the simulation depends on the enzyme concentration as a hyperbolic function (Fig. 6), in accordance with the calculation presented above (Eq. 12).

### Sensitivity of kinetic simulations to kinetic parameters ( $a$ , $b$ , $c$ , and $d$ ) in the case of the autocatalytic triangular model

The effects of different kinetic parameters in the case of partially activated hydrogenase are to be seen in Fig. 7. An arbitrary kinetic parameter set ( $a = 0.001$ ,  $b = 100$ ,  $c = 100$ ,  $d = 10^{-10}$ ), and initial parameters ( $E_T = 10^4$ ,  $E_1 = (1 - 0.00001) \cdot E_T$ ,  $E_2 = 0$ ,  $E_3 = 0.00001 \cdot E_T$ ,  $E_4 = 0$ ,  $H_{20} = 10^6$ ,  $p_0 = 0$ ,  $M_o = 400$ ) were chosen and the kinetic curves were calculated for this parameter set and also on changing all kinetic constants separately by one order of magnitude both up and down.

As in the discussion of Eqs. 10 and 11,  $a$  is found experimentally to be small ( $\sim 0.001$ – $0.0001 \text{ s}^{-1}$ ) (5,11,16). If we decrease the parameter from the initial value (0.001) to  $0.0001 \text{ s}^{-1}$ , which is still within the measured range, the lag phase becomes more characteristic. Increasing this parameter lowers the lag phase and smoothes the acceleration of the activity. When we increase this parameter infinitely (activating the enzyme,  $a = \infty$ ), then, to make the lag phase observable, the total enzyme concentration should be decreased as well (Fig. 3).

Changing parameter  $d$  has the opposite effect from that for  $a$ . Decreasing  $d$  causes the enzyme form  $E_4$  to accumulate with decreases in both enzyme forms  $E_3$  and  $E_2$ . Consequently, the lag phase characteristic is more pronounced at high values of kinetic constant  $d$ . Moreover, the activity of the enzyme is proportional to  $d$  (see Eqs. 5 and 8 and Fig. 7).

It may be concluded from Eqs. 9 and 11, that kinetic constants  $b$  and  $c$  have opposite effects. Decreasing  $b$  and/or increasing  $c$  emphasizes the lag phase characteristic of the reaction. The kinetics are sharper, and the acceleration of the reaction is much higher. In contrast increasing  $b$  and/or decreasing  $c$  makes the lag phase characteristic more smooth; the lag phase may even diminish if the change is high. In fact, the ratio  $c/b$  is important (see Eqs. 9 and 11): it determines whether the autocatalytic nature of the reaction can be seen or not. If  $c/b$  is very small (the autocatalytic reaction  $b$  is very fast), the whole autocatalytic reaction becomes negligible and unobservable. However, there is a very wide gap, of more than three orders of magnitude in the numerical values of the kinetic parameters, between which the autocatalytic nature of the reaction is pronounced at a given enzyme concentration.

The parameter values used in the kinetic simulations were chosen so as to furnish the closest resemblance between the real experiments with the simulated experiments they produce.

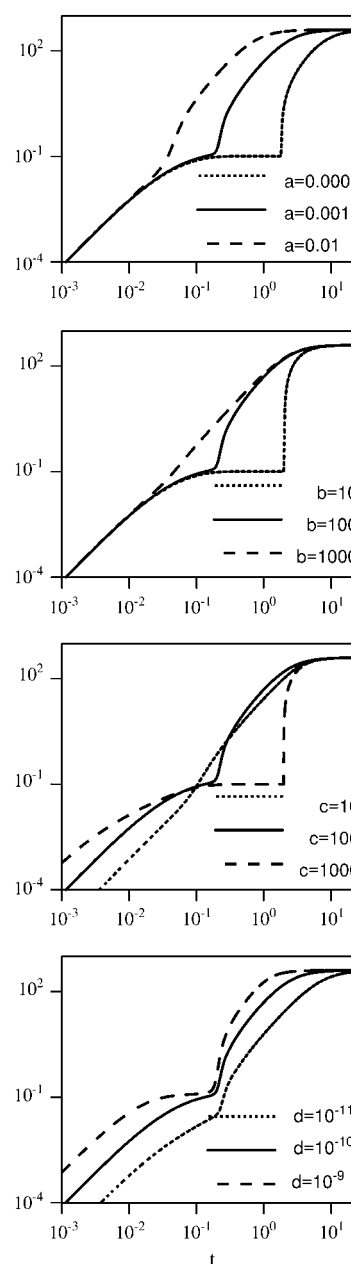


FIGURE 7 The sensitivity of the resulted kinetic curves on changing the kinetic parameters. An arbitrary kinetic parameter set ( $a = 0.001$ ,  $b = 100$ ,  $c = 100$ ,  $d = 10^{-10}$ ), and initial parameters ( $E_T = 10^4$ ,  $E_1 = (1 - 0.00001) \cdot E_T$ ,  $E_2 = 0$ ,  $E_3 = 0.00001 \cdot E_T$ ,  $E_4 = 0$ ,  $H_{20} = 10^6$ ,  $p_0 = 0$ ,  $M_o = 400$ ) were chosen and the kinetic curves were calculated. Each kinetic constant was separately changed to 10 times higher and 10 times lower values and the kinetic curves were calculated again. The results are plotted for kinetic constants  $a$ ,  $b$ ,  $c$ , and  $d$ , respectively. All kinetic curves are in log-log representation.

## DISCUSSION

### Measurement of hydrogenase activity

We have previously demonstrated that the hydrogenase cycle contains at least one autocatalytic step. It is most likely

that the autocatalytic step occurs between two different enzyme forms (13–15). The theoretical calculations provide more evidence about the relevance of the autocatalytic model and explain some of the characteristics of the hydrogenase activity.

The lag phase dependence on the enzyme concentration is a typical feature of the autocatalytic behavior of the enzyme reaction model. The lag phase in our model system has two sources. The conventional lag phase is due to the slow “activation” process ( $E_1$  to  $E_2$ ); it is small and it does not depend on the enzyme concentration. The other lag phase, which is due to the introduction of an autocatalytic step, however, can be very long and depends on the enzyme concentration.

We have previously observed that the enzyme reaction has a lag phase and that this lag phase is concentration dependent for both inactive and active enzyme forms (15,17). The measured lag phase versus enzyme concentration dependence was best described by a hyperbolic function that is in excellent agreement with the theoretical predictions (Figs. 2, 3, and 6 and Eq. 12).

Unfortunately, very few other experiments have been reported in which this feature of the enzyme reaction was investigated. The interconversion of different enzyme forms has been followed by stopped-flow IR (9). A ready enzyme form (Form B) was reacted with hydrogen gas to determine the characteristics of the reaction. It was concluded that neither the lag phase (6 s at 40  $\mu\text{M}$ , 7 s at 20  $\mu\text{M}$ , and 11 s at 10  $\mu\text{M}$  enzyme) nor the initial rate ( $t_{1/2} = 9$  s at all enzyme concentrations) of the reaction depends on the enzyme concentration. Although there are few points, it is possible to fit a hyperbolic function to the data provided (Fig. 8). The fit is even better if we reevaluate the data from the published picture. The reevaluated data are slightly different, but, because the experiment is very noisy, the published and reevaluated data are within the experimental error. We can

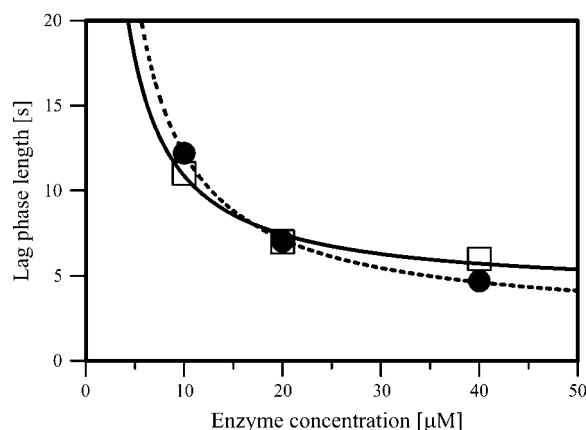


FIGURE 8 Enzyme concentration dependence of lag phase of *Allochromatium vinosum* hydrogenase. The picture was calculated from Fig. 5 in Kurkin et al. (9). (□) Data provided by the authors in the text; (●) reevaluated data. A hyperbolic function (power  $-1$ ) was fitted to both curves.

state that this experiment supports, or at least does not contradict, our autocatalytic model.

It has also been stated previously that the enzyme activity displays a concentration dependence (2,17–19). From theoretical calculations and model simulations, it is evident that this behavior is not a consequence of the autocatalytic step because it is found for the conventional model as well. The dependence can be explained by the fact that the active enzyme concentration during the enzyme assay continuously increases due to the slow “activation” of the enzyme. This is described in our model as a very slow conversion of enzyme form  $E_1$  to  $E_2$ , which can be simplified as a continuous increase in  $E_a$ . The overall reaction, which is limited by the amount of the substrate, is much faster than the conversion of  $E_1$  to  $E_2$ , and the maximum velocity of the reaction (the activity of the enzyme) therefore depends on the enzyme concentration. If we activate the enzyme ( $E_1 = 0$ ), the enzyme concentration dependence of the activity disappears in both the autocatalytic and the nonautocatalytic model.

### Activation of hydrogenase

When isolated, hydrogenase is in its “inactive” forms. The “as purified” enzyme from *T. roseopersicina* contains 80% Form B ( $\text{Ni}_\text{r}\text{-B}_{1943}^*$  in Fig. 1) and 20% Form A ( $\text{Ni}_\text{u}\text{-A}_{1945}^*$  in Fig. 1) (20), whereas for *Desulfovibrio gigas* the distribution is  $\sim 30\%$  Form B and 70% Form A (5,11). The actual distribution of the inactive enzyme forms depends on the particular enzyme, the purification circumstances, etc.

It is known that hydrogenase needs to be activated to attain a higher activity (5,16). Activation can be achieved by the

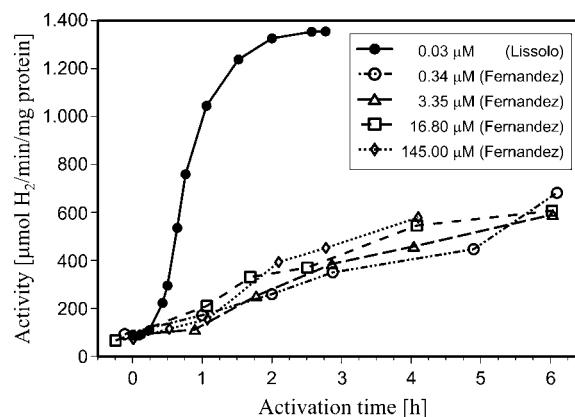


FIGURE 9 Activation of hydrogenase from *D. gigas*. The picture was combined from the publications of Lissolo et al. (16) and Fernandez et al. (5). At the lowest enzyme concentration (0.03  $\mu\text{M}$ ; measurement from Lissolo et al. (16)), the lag phase of the activation is clearly seen. The lag phase is  $\sim 15$ –20 min, after which the activity increases rapidly. No lag phase could be observed in the case of the measurements from Fernandez et al. (5). We should mention that the enzyme concentrations in this case were at least 10 times higher than in measurements from Lissolo et al. (16) and the first measurements were performed 1 h after the start of activation, with the only exception of the highest enzyme concentration, where the first sample was withdrawn after incubation for 30 min. This time is much longer than the lag phase for the lowest enzyme concentration ( $\sim 20$  min).

incubation of hydrogenase under a hydrogen atmosphere. The activation of hydrogenase starts with a lag phase (11,16), which is concentration dependent (Fig. 9). We have demonstrated that only the autocatalytic, and not the conventional model can describe the observed lag phase of the activation (Fig. 2).

Activation is routinely used to determine hydrogenase activity (11). Besides the fact that the measured activity of the enzyme increases, however, there is no clear evidence as to what the activation means. It is suggested that "activation" involves the removal of an oxygen molecule or an oxygen compound bound to or near the catalytic center (21) and/or one-electron reduction of the inactive forms (7,21).

We suggest that "activation" in the case of hydrogenase is a twofold process. The first step is the removal of the oxygen and/or an oxygen compound from the active site (21). This can be achieved by incubating the enzyme under anaerobic conditions or through any process that removes the oxygen. Strictly speaking, this is the real activation of the hydrogenase because, after removal of the oxygen species, the enzyme is in a form that is already part of the enzyme cycle. It is also possible that, to remove oxygen, it is necessary to reduce the enzyme by one or two electrons.

The second step of the "activation" involves the redistribution of the enzyme forms in the enzyme cycle, producing an available amount of a hydrogen-bound enzyme form that can interact autocatalytically with another enzyme form that does not bind hydrogen. The end product of this "activation" is Form SR, after which further reaction in the enzyme cycle is blocked: the second substrate, the electron acceptor, is missing from the reaction and its absence prevents completion of the enzyme cycle. We may postulate that Form SR is the enzyme form that interacts with the electron acceptor and that one of the autocatalytic partners takes place before the Form SR in the reaction cycle.

Because a lag phase dependence may be observed in both the inactive and active hydrogenase forms (9,15,17), we can conclude from theoretical simulations that the autocatalytic step is part of the enzyme cycle. This is in good agreement with the experimental findings of special patterns during the hydrogenase-uptake reaction in a thin-layer reaction chamber and of autocatalytic oscillations in the fast absorption kinetics of the methyl viologen-initiated reaction of hydrogenase (13–15).

This work was supported by the Hungarian Science Foundation (OTKA T 029008, OTKA M45378, OTKA T 049276, and OTKA-NSF 35540). R.M.M.B. acknowledges the support of the Portuguese Science and Technology Foundation under the PhD fellowship of POCTI, SFRH/BD/13128/2003, and the European Social Fund through "III Quadro Comunitário de Apoio".

## REFERENCES

1. Fisher, H. F., A. I. Krasna, and D. Rittenberg. 1954. The interaction of hydrogenase with oxygen. *J. Biol. Chem.* 209:569–578.
2. Krasna, A. I., and D. Rittenberg. 1954. The mechanism of action of the enzyme hydrogenase. *J. Am. Chem. Soc.* 76:3015–3020.
3. Anand, S. R., and A. I. Krasna. 1965. Catalysis of the H<sub>2</sub>-HTO exchange by hydrogenase. A new assay for hydrogenase. *Biochemistry*. 4:2747–2753.
4. Yagi, T., M. Tsuda, and H. Inokuchi. 1973. Kinetic studies on hydrogenase. Parahydrogen-orthohydrogen conversion and hydrogen-deuterium exchange reactions. *J. Biochem. (Tokyo)*. 73:1069–1081.
5. Fernandez, V. M., E. C. Hatchikian, and R. Cammack. 1985. Properties and reactivation of two different deactivated forms of *Desulfovibrio gigas* hydrogenase. *Biochim. Biophys. Acta*. 832:69–79.
6. De Lacey, A. L., J. Moiroux, and C. Bourdillon. 2000. Simple formal kinetics for the reversible uptake of molecular hydrogen by [Ni-Fe] hydrogenase from *Desulfovibrio gigas*. *Eur. J. Biochem.* 267:6560–6570.
7. Vignais, P. M., L. Cournac, E. C. Hatchikian, S. Elsen, L. T. Serebryakova, N. A. Zorin, and B. Dimon. 2002. Continuous monitoring of the activation and activity of [NiFe]-hydrogenases by membrane-inlet mass spectrometry. *Int. J. Hydrogen Energy*. 27:1441–1448.
8. Armstrong, F. A. 2004. Hydrogenases: active site puzzles and progress. *Curr. Opin. Chem. Biol.* 8:133–140.
9. Kurkin, S., S. J. George, R. N. F. Thorneley, and S. P. J. Albracht. 2004. Hydrogen-induced activation of the [NiFe]-hydrogenase from *Allochromatium vinosum* as studied by stopped-flow infrared spectroscopy. *Biochemistry*. 43:6820–6831.
10. Albracht, S. P. J. 2001. Spectroscopy: the functional puzzle. In *Hydrogen as a Fuel: Learning from Nature*. R. Cammack, M. Frey, and R. Robson, editors. Taylor and Francis, London, UK; New York, NY.
11. Cammack, R. 2001. Hydrogenases and their activities. In *Hydrogen as a Fuel: Learning from Nature*. R. Cammack, M. Frey, and R. Robson, editors. Taylor and Francis, London, UK; New York, NY.
12. De Lacey, A. L., C. Stadler, C. Cavazza, E. C. Hatchikian, and V. M. Fernandez. 2000. FTIR characterization of the active site of the Fe-hydrogenase from *Desulfovibrio desulfuricans*. *J. Am. Chem. Soc.* 122:11232–11233.
13. Ósz, J., and C. Bagyinka. 2001. Experimental evidence for autocatalytic reaction cycle of hydrogenase enzyme. *Eur. J. Biochem.* 268 (Suppl. 1).
14. Bagyinka, C., J. Ósz, and S. Száraz. 2003. Autocatalytic oscillations in the early phase of the photoreduced methyl viologen-initiated fast kinetic reaction of hydrogenase. *J. Biol. Chem.* 278:20624–20627.
15. Ósz, J., and C. Bagyinka. 2005. An autocatalytic step in the reaction cycle of hydrogenase from *Thiocapsa roseopersicina* can explain the special characteristics of the enzyme reaction. *Biophys. J.* 89:1984–1989.
16. Lissolo, T., S. Pulvin, and D. Thomas. 1984. Reactivation of the hydrogenase from *Desulfovibrio gigas* by hydrogen: influence of redox potential. *J. Biol. Chem.* 259:11725–11729.
17. Dér, A., C. Bagyinka, T. Páli, and K. L. Kovács. 1985. Effect of enzyme concentration on apparent specific activity of hydrogenase. *Anal. Biochem.* 150:481–486.
18. Kleiner, D., and R. H. Burris. 1970. The hydrogenase of *Clostridium pasteurianum*. Kinetic studies and the role of molybdenum. *Biochim. Biophys. Acta*. 212:417–427.
19. Bagyinka, C., N. A. Zorin, and K. L. Kovacs. 1984. Unconsidered factors affecting hydrogenase activity measurement. *Anal. Biochem.* 142:7–15.
20. Bagyinka, C., J. P. Whitehead, and M. J. Maroney. 1993. An X-ray absorption spectroscopic study of nickel redox chemistry in hydrogenase. *J. Am. Chem. Soc.* 115:3576–3585.
21. Lamle, S. E., S. P. J. Albracht, and F. A. Armstrong. 2004. Electrochemical potential-step investigations of the aerobic interconversions of [NiFe]-hydrogenase from *Allochromatium vinosum*: insights into the puzzling difference between unready and ready oxidized inactive states. *J. Am. Chem. Soc.* 126:14899–14909.